RADIOISOTOPES, **46**, 603–614 (1997)

Intermittent Measurements of ^{222}Rn and ^{220}Rn Progeny in Air for Four Years

Tsuneo KOBAYASHI and Yuji TAKAKU

Department of Physics, Fukushima Medical College
1, Hikarigaoka, Fukushima-shi 960-12, Japan

Received 13, January 1997

To survey the level and behavior of ^{222}Rn and ^{220}Rn progeny in air, measurements were made intermittently (once a day at an identical time) for 4 years at the campus of the authors' college located in the northeastern part of Japan. A filtration method with alpha spectroscopy, using an evacuated chamber, clearly separated ^{212}Po peak from others. Outdoor and indoor air were sampled every morning except holidays. A definite seasonal variation, higher concentrations in autumn and in winter, was observed except indoor ^{220}Rn progeny. ^{222}Rn progeny revealed log-normal distribution, whereas ^{220}Rn progeny revealed Poisson-like distribution. Multiple regression analysis and correlation analysis indicated that most of indoor ^{222}Rn progeny originates from outdoor air. From time series analysis, several-day periods were often observed, which will probably be attributed to the wind speed.

Key Words: radon, thoron, progeny, daily variation, concentration in ambient air, multiple regression analysis, time series analysis, spectral analysis

1. Introduction

Investigations have been made on ^{222}Rn and ^{220}Rn progeny in air at the campus of the authors' college located in the northeastern part of Japan (37°45′ N, 140°28′ E, 67.4 m above sea level). Generally, annual effective dose equivalent of a human body in natural environment is known to be about 2 mSv, and about half of which is due to internal exposure to ^{222}Rn and ^{220}Rn progeny. Therefore, clarifying the behavior of these decay products is an issue of wide importance to radiation protection, etc. The aim of the present research was to survey the level and behavior of ^{222}Rn and ^{220}Rn progeny at the authors' campus. Measurements were performed from December 1988 to June 1993 using alpha spectroscopic method[1)-3)]. Statistical and time-series analyses for those data compiled have obtained a few interesting results.

2. Materials and Methods

A filtration method with alpha spectroscopy was employed for the measurement of ^{222}Rn and ^{220}Rn progeny concentration[2)]. Membrane filters (Advantec A080A055C, pore size : 0.8 μm) were used. Collection efficiency of the filters was assumed to be unity. A self-contained alpha spectrometer (ORTEC 676) was used, which consists of a silicon surface-barrier semiconductor detector (active area : 900 mm^2, thickness of depletion layer : 100 μm), a preamplifier, a vacuum chamber, etc. Distance between the filter and the detector was 10 mm. Emerging efficiency was assumed as 0.98 following the report of James et al.[4)]. Counting efficiency was estimated as 0.125. After 10 min sampling (20 l min^{-1}) of the progeny in air, 2 min were required to set the

filter to the vacuum chamber containing semiconductor detector. The activity on the filter was detected for every ten minutes for five counting intervals, and the results were recorded on a personal computer. The aims of 5 counting intervals are that a comparison with the often-used gross-alpha three-count method is possible, and that a least-squares fit may be possible. By using an evacuated chamber, ^{212}Po (ThC′) peak (8.78 MeV) was clearly separated from others. To confirm the stability of the measuring system, energy- and yield-calibration with ^{241}Am standard source (5.55 kBq) was performed once a week.

Figure 1 shows a typical alpha spectra for the five counting interval. The alpha spectrum was divided into three regions : ^{218}Po (RaA)+^{212}Bi (ThC) region (4.6 to 6.2 MeV), ^{214}Po (RaC′) region (6.2 to 7.9 MeV), and ^{212}Po (ThC′) region (7.9 to 9.3 MeV). Interferences between these three regions were negligible, especially because

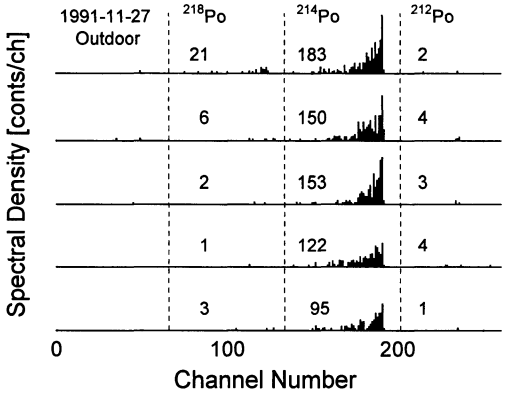

Fig. 1 Typical alpha spectra used to obtain ^{222}Rn- and ^{220}Rn-progeny concentrations.
The first counting starts 2 min after the end of 10 min sampling of air. Dashed lines separates three regions of interest, i.e., ^{218}Po (RaA) region (4.6 to 6.2 MeV), ^{214}Po (RaC′) region (6.2 to 7.9 MeV), and ^{212}Po (ThC′) region (7.9 to 9.3 MeV).

of few counts of ^{212}Po region. Three ^{222}Rn progeny, ^{218}Po, ^{214}Pb, ^{214}Bi, concentrations were obtained from the three counts, i.e., counts of the first ^{214}Po region, counts of the first ^{218}Po region and counts of the sum of the second to fifth ^{214}Po region. The potential alpha energy concentration (PAEC) of ^{222}Rn progeny, PAEC(^{222}Rn), was calculated from these three concentrations. As a representative variable of progeny concentrations, PAEC was adopted in the present work, because of the convenience of statistical analyses and because of the possibility of effective dose estimates in future. ^{220}Rn progeny concentration, PAEC (^{220}Rn), was estimated from the sum of the five counts of ^{212}Po region. The ratio of ^{212}Pb : ^{212}Bi was assumed as 1 : 1, 1 : 0.6, and 1 : 0.3 ; the three values were averaged into PAEC(^{220}Rn). Lower detection limits were 0.4 nJ m^{-3} for ^{222}Rn and 2 nJ m^{-3} for ^{220}Rn progeny, respectively.

Measurements were made for outdoor (from 9 : 10 to 9 : 20 a.m.) and indoor (from 10 : 10 to 10 : 20 a.m.) air every day except holidays, taking into account that measurements at the identical times are essentially indispensable for time-series analysis, and that the activity of people is done in approximately the same time zone regardless of the seasons. Outdoor air was sampled on the fourth floor of an emergency staircase. Indoor air was sampled around the authors' office, which is on the fourth floor of a five storied building. The college building was built in 1988.

3. Results and Discussion

3・1 Basic statistics and seasonal variation

Table 1 shows basic statistical quantities of ^{222}Rn and ^{220}Rn progeny. Indoor ^{222}Rn-progeny level is less than that of outdoor, probably because of the ventilation system which draws outdoor air into indoor through some filters[3].

Figure 2 shows plots of raw data of ^{222}Rn and

Table 1 Basic statistical quantities for ^{222}Rn and ^{220}Rn progeny

	Outdoor		Indoor	
	PAEC*(^{222}Rn)	PAEC(^{220}Rn)	PAEC(^{222}Rn)	PAEC(^{220}Rn)
Number	1 100	1 100	1 050	1 050
Average	19.3	4.3	11.4	4.9
Standard deviation	12.5	5.6	6.7	4.3
Maximum	83.8	52.5	50.7	22.8
Minimum	2.5	0	1.7	0
Median	15.8	2.3	9.7	4.4
Rate of >0**	100%	66%	100%	82%

* PAEC denotes potential alpha energy concentration in units of nJ m^{-3}.
** Rate of >0 means the ratio of positive data to total data in %.

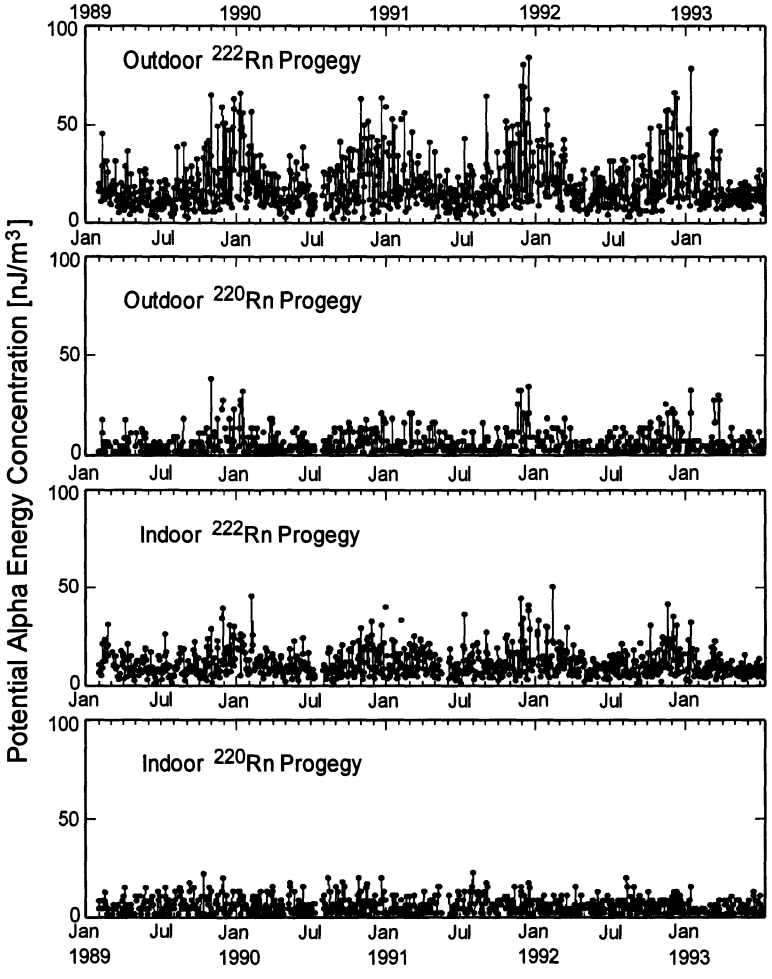

Fig. 2 Plots of raw data of outdoor and indoor atmospheric ^{222}Rn- and ^{220}Rn-progeny concentrations (potential alpha energy concentration, PAEC). The abscissa represents days from 1 January 1989, and the ordinate represents PAEC. Indoor ^{222}Rn progeny level is less than that of outdoor. Clear seasonal variation is seen except indoor ^{220}Rn progeny.

Table 2 Seasonal average of several ratios concerning ^{222}Rn progeny and PAECs in nJ m^{-3}

Season	Outdoor					Indoor				
	B/A	C/A	$\frac{A}{B+C}$	PAEC (^{222}Rn)	PAEC (^{220}Rn)	B/A	C/A	$\frac{A}{B+C}$	PAEC (^{222}Rn)	PAEC (^{220}Rn)
Spring	0.67	0.72	0.22	16.0	3.6	0.47	0.41	0.37	10.6	4.2
Summer	0.77	0.85	0.19	14.4	3.3	0.19	0.22	0.36	9.4	5.6
Autumn	0.70	0.62	0.19	22.2	5.1	0.40	0.47	0.35	12.3	5.3
Winter	0.73	0.71	0.21	25.3	5.2	0.45	0.46	0.33	13.6	4.7

B/A, C/A, and A/(B+C) denote the ratio of ^{214}Pb to ^{218}Po, the ratio of ^{214}Bi to ^{218}Po, and the ratio* of PAEC from ^{218}Po to PAEC from ^{214}Pb and ^{214}Bi, respectively. Spring, summer, autumn, and winter denote March to May, June to August, September to November, and December to February, respectively.

* Under the equilibrium conditions, the PAEC rations of B/A, C/A and A/(B+C) are about 4.94, 3.66, and 0.116, respectively.

^{220}Rn progeny ; the abscissa represents days from January 1, 1989, and the ordinate represents PAEC.

A definite seasonal variation, i.e., higher concentrations in autumn and in winter, was observed every year for outdoor and indoor ^{222}Rn progeny and outdoor ^{220}Rn progeny. This tendency was not so clear for indoor ^{220}Rn progeny.

Table 2 shows seasonal average of ratios and concentrations. As to ^{222}Rn progeny, concentrations of three decay products were obtained, and the ratio of ^{214}Pb to ^{218}Po, the ratio of ^{214}Bi to ^{218}Po, and the ratio of PAEC from ^{218}Po to PAEC from ^{214}Pb and ^{214}Bi were obtained. Ratios in Table 2 indicate that the air was fresher in indoor than in outdoor.

3·2 Statistical distribution

Figure 3(a) shows log-normal plots of ^{222}Rn and ^{220}Rn progeny. All progeny appears to fit log-

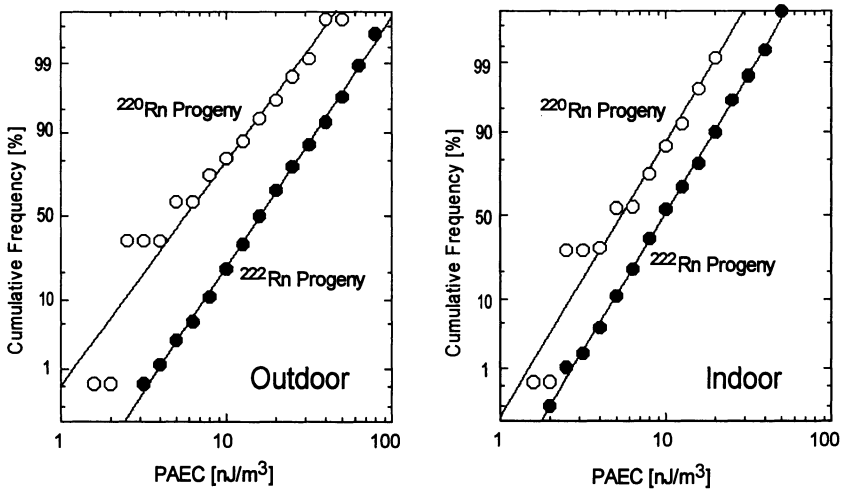

Fig. 3(a) Log-normal plots of cumulative frequency, where zero data of ^{220}Rn progeny are omitted.
Apparently, all progeny seems to fit log-normal distribution, however it is not true (see next figure).

normal distribution, however log-normal plot is not always a good way for this judgment. In fact, a chi-square test with a significant level of 1% indicated that ^{222}Rn progeny did fit log-normal distribution, while ^{220}Rn progeny did not.

Figure 3 (b) shows frequency distributions of the progeny concentrations. ^{222}Rn progeny revealed certainly log-normal distribution, while ^{220}Rn progeny revealed Poisson-like rather than log-normal distribution, though another chi-square test indicated that ^{220}Rn progeny fits neither log-normal nor Poisson distribution. The Poisson-like distribution may be attributed to the low level of ^{220}Rn progeny.

3・3 Multiple regression analysis

In order to reveal the factors which causes the variation of ^{222}Rn progeny, multiple regression analysis was made for outdoor and indoor data from December 1988 to December 1990.

First, stepwise multiple regression analysis was made for outdoor ^{222}Rn progeny concentration as a dependent variable, and outdoor temperature, outdoor humidity, atmospheric pressure and wind speed as candidates of independent variables. The result picked up outdoor temperature, one of the good index of convectional stability of the environmental air, and wind speed as suitable independent variables. Second, the same stepwise multiple regression analysis was made for indoor ^{222}Rn progeny concentration as a dependent variable, and outdoor temperature, indoor temperature, outdoor humidity, indoor humidity, atmospheric pressure and wind speed as candidates of independent variables. The result picked up again outdoor temperature and wind speed as suitable independent variables. This last result seems interesting, since outdoor parameters explain indoor ^{222}Rn progeny.

The result of the regression analysis was interpreted as follows. ^{222}Rn (half life 3.82 days) is an inert gas 7.5 times as heavy as air; its origin is radium (^{226}Ra, half life 1 600 year). ^{222}Rn progeny level is roughly in proportion to ^{222}Rn level. Al-

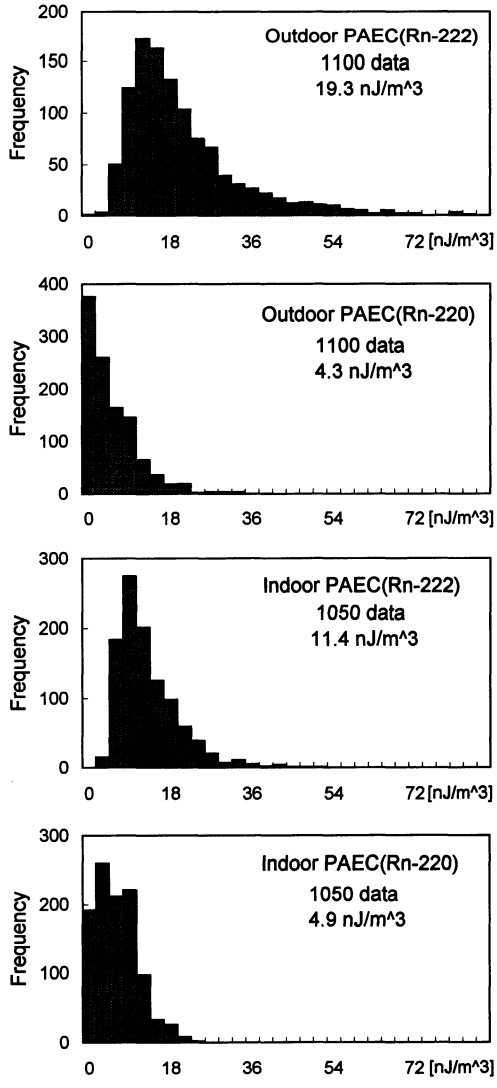

Fig. 3(b) Histogram of progeny concentrations.
^{222}Rn progeny reveals certainly log-normal distribution, while ^{220}Rn progeny reveals Poisson rather than log-normal distribution. The Poisson distribution may be attributed to the low level of ^{220}Rn progeny.

though the activity of radium is not affected by vertical distribution of air temperature or wind speed, the vertical transport of emanated ^{222}Rn above the earth's surface is affected by convectional stability of the environmental air and large wind speed. Therefore, the result that outdoor ^{222}Rn progeny is affected by outdoor temperature and wind speed is quite reasonable. On the other hand, why indoor ^{222}Rn progeny is affected by outdoor parameters? That may be probably because the ^{222}Rn in air of the laboratory of the authors mostly originates from outdoor.

In fact, the office of the authors adopts ventilation system which draws outdoor air into indoor through some filters. Due to this ventilation system, indoor ^{222}Rn progeny level is lower than that of outdoor. However, this ventilation system is not able to capture inert ^{222}Rn gas. The ^{222}Rn gas from outdoor decays into progeny in indoor. Thus the dominant origin of indoor ^{222}Rn progeny is considered to be the outdoor ^{222}Rn gas drawn into indoor.

This interesting result for indoor ^{222}Rn progeny will be supported from the next correlation analysis for ^{222}Rn and ^{220}Rn progeny.

The reason why outdoor temperature and wind speed were suitable independent variables will become clearer from the following time series analysis. As can be seen from Fig. 6, outdoor temperature had overwhelming one-year period of variation, and from Fig. 7, wind speed had strong several-day periods of variation. Additionally, outdoor temperature and wind speed had no correlation. Thus, looking data from multiple regression analysis in time scale of about two years, outdoor temperature and wind speed were probably two of the most suitable variables to explain variations of ^{222}Rn progeny.

3·4 Correlation analysis

Figure 4 shows scatter diagrams for ^{222}Rn and ^{220}Rn progeny in outdoor and indoor air using data from 3 July 1989 to 26 November 1990. The correlation coefficients (R) between outdoor and indoor air were 0.79(**) for ^{222}Rn progeny and 0.15(*) for ^{220}Rn progeny, respectively. The symbol, (**) and (*), mean that the p-value[5] is less than 1 % and 5 %, respectively. The concentration of ^{222}Rn progeny in indoor air is highly correlated to that in outdoor air, however it is not the case for ^{220}Rn progeny. This may be attributed to the short half life of ^{220}Rn (55 s); the probabil-

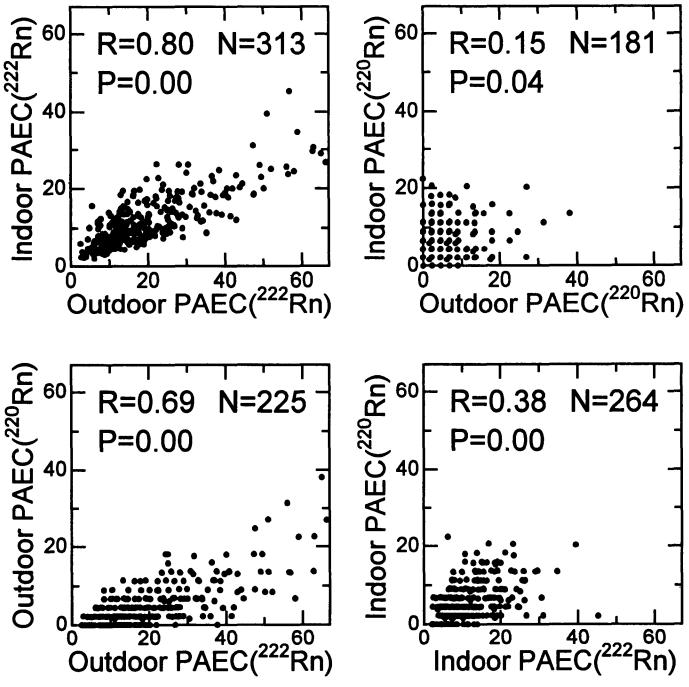

Fig. 4 Scatter diagram of outdoor and indoor atmospheric ^{222}Rn- and ^{220}Rn-progeny concentrations.
Top : indoor versus outdoor. Bottom : ^{220}Rn progeny versus ^{222}Rn progeny.

Table 3 Pearson correlation coefficients for ^{222}Rn and ^{220}Rn progeny concentraions and meteorological data (in parentheses are number of data)

	Outdoor		Indoor	
	PAEC(^{222}Rn)	PAEC(^{220}Rn)	PAEC(^{222}Rn)	PAEC(^{220}Rn)
Outdoor temperature	−0.2621 (330) p=0.000	−0.1825 (224) p=0.006	−0.2747 (312) p=0.000	0.0550 (264) p=0.373
Indoor temperature	−0.1559 (314) p=0.006	−0.1722 (211) p=0.012	−0.1972 (313) p=0.000	−0.0625 (265) p=0.310
Wind speed	−0.4337 (330) p=0.000	−0.2001 (224) p=0.003	−0.3708 (312) p=0.000	−0.0338 (264) p=0.585
Atmospheric pressure	0.2994 (330) p=0.000	0.2539 (224) p=0.000	0.2471 (312) p=0.000	−0.0610 (264) p=0.323

ity for the introduction of outdoor ^{220}Rn is less than that of outdoor ^{222}Rn.

The correlation coefficients between ^{222}Rn progeny and ^{220}Rn progeny were 0.69(**) for outdoor air and 0.38(**) for indoor air, respectively. ^{222}Rn progeny was usually accompanied with ^{220}Rn progeny in outdoor air, however it is not the case in indoor air. This may indicate that most indoor ^{222}Rn comes from outdoor air, while few indoor ^{220}Rn comes from outdoor air.

From these correlation analyses and the regression analyses of the previous section, most of indoor ^{222}Rn progeny at the authors' office seems to be originated from ^{222}Rn gas drawn from outdoor air.

Table 3 shows correlations between progeny concentrations and a few meteorological data. Interestingly, indoor ^{220}Rn progeny showed no correlation with meteorological data, while other progeny showed similar correlation with meteorological data; negative correlation with outdoor and indoor temperature, negative correlation with wind speed, and positive correlation with atmospheric pressure. No correlation between outdoor temperature and wind speed was observed ($R=-0.0050$, $p=0.93$), while negative correlation was observed between wind speed and atmospheric pressure ($R=-0.1971$, $p=0.00$). Negative correlation between wind speed and atmospheric pressure supports the positive correlation between progeny concentrations and atmospheric pressure.

3·5 Time series (spectral) analysis

Temporal variation of ^{222}Rn and ^{220}Rn progeny concentration was studied in detail with several information — theoretical methods such as autocorrelation, Fourier transform, autoregressive model, etc. Figure 2 shows that the progeny concentration changes considerably from day to day. The concentration is regarded as a random variable rather than continuous variable of time. Therefore, considering progeny concentration as a time series signal, spectral analyses were made on the temporal variation of progeny concentration. Details of the analyses are shown in appendix.

Figure 5 shows typical power spectra of outdoor ^{222}Rn progeny concentration as an example.

The upper figure shows a logarithm plot of ^{222}Rn progeny concentration, and the lower figure shows the power spectrum from autoregressive model which is equivalent to maximum entropy method. Used data were from 7 August 1989 to 26 May 1992. The order of autoregressive model was set as $m=33$ (see appendix). One-year period was clearly identified as mentioned previously. Besides the one year period, 3- to 9-day periods were often observed. Other progeny concentrations also showed the similar power spectra as Fig. 5.

The same time-series analysis was made for meteorological data. Figures 6, 7, and 8 show results of outdoor temperature, wind speed, and atmospheric pressure, respectively. Outdoor temperature showed an overwhelming one-year period, while wind speed showed strong several-day periods. Again, temperature and wind speed seem to affect progeny concentrations considerably.

Figures 5 to 8 show peaks of 21- to 26-day period. This may be attributed to meteorological phenomena corresponding to the rotation period of the sun. Approximately the same periodicity was pointed out by Minato[6]; he suggested that a 20-day periodicity exists sometimes in radon progeny and meteorological quantity.

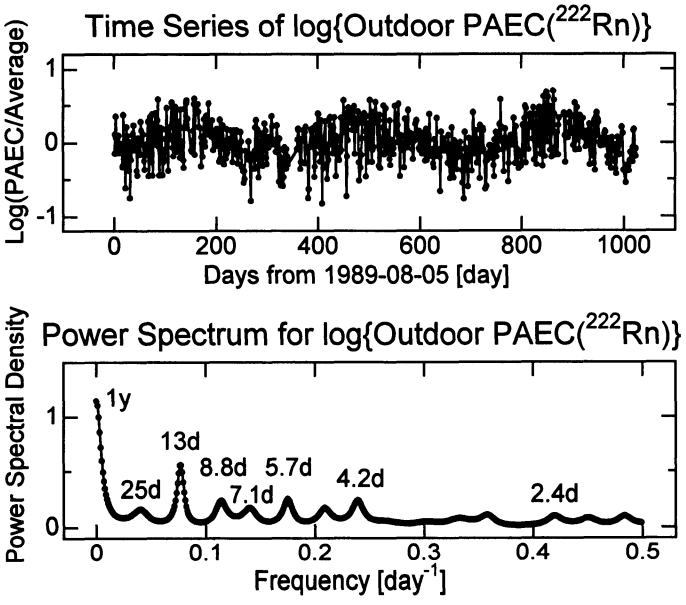

Fig. 5 Time-series analysis for outdoor ^{222}Rn progeny concentration.
Top : logarithm plot of PAEC(^{222}Rn)/average. Bottom : power spectrum deduced from autoregressive model which is equivalent to maximum entropy method. Besides the one year period, 3- to 9-day periods were often observed.

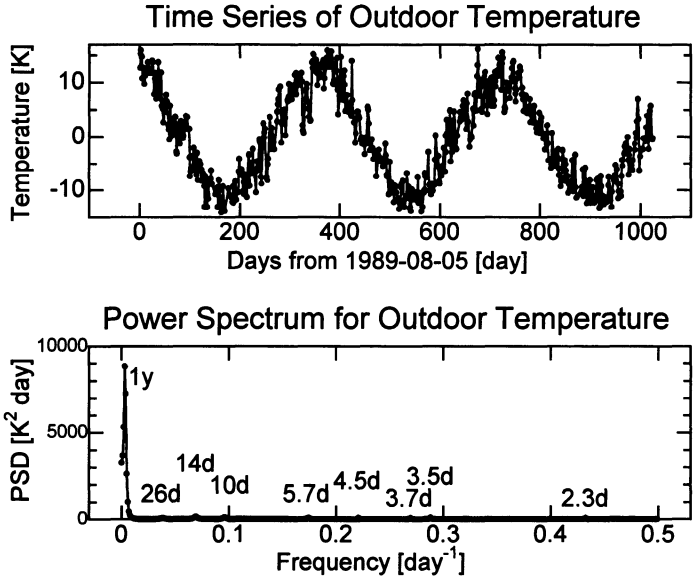

Fig. 6 Time-series analysis for outdoor temperature.
Top : plot of deviation from average. Bottom : power spectrum deduced from autoregressive model ; PSD means power spectral density. One-year period is overwhelming.

4. Concluding Remarks

Based on the data of ^{222}Rn and ^{220}Rn progeny in air, statistical and time-series analyses were made. The present indoor data might be a singular case, whereas the outdoor data is probably a well seen case in Japan showing an interesting temporal variation.

Since the present data are from intermittent measurements, the observed seasonal variation, e.g., might be only the reflection of the meteorological condition about the time of the measurements. Furthermore, whether the data measured at 9 : 15 or 10 : 15 are proportional to the mean progeny concentration of the day is yet unknown (see the first Appendix and Fig. 6). Investigations concerning these problems are left in the future study.

Appendix

Diurnal dependence

Typical diurnal dependence of outdoor ^{222}Rn and ^{220}Rn progeny on a sunny winter day is shown in Fig. 9. Well-known behavior, i.e., higher level in the morning and lower level in the evening, was observed, also for ^{220}Rn progeny.

Details of spectral analyses[7),8)]

Autocorrelation function (ACF) for random signal, $x(t)$, is defined as

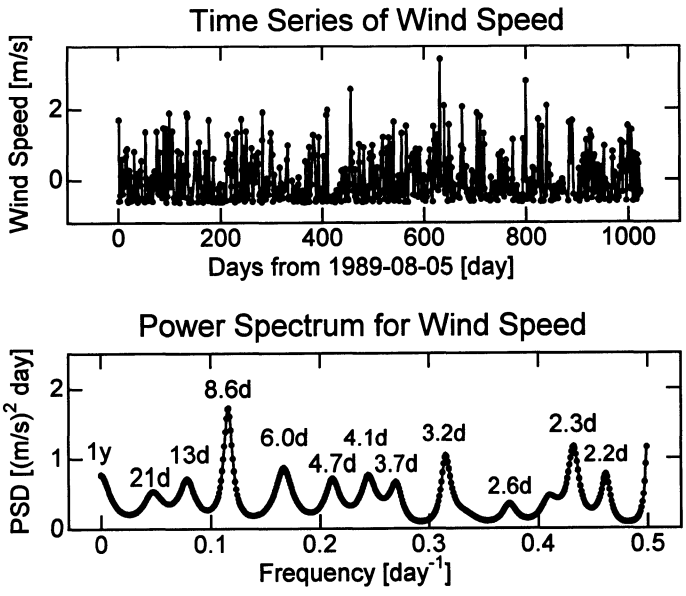

Fig. 7 Time-series analysis for wind speed.
Top : plot of deviation from average. Bottom : power spectrum deduced from autoregressive model. Strong several-day periods are seen.

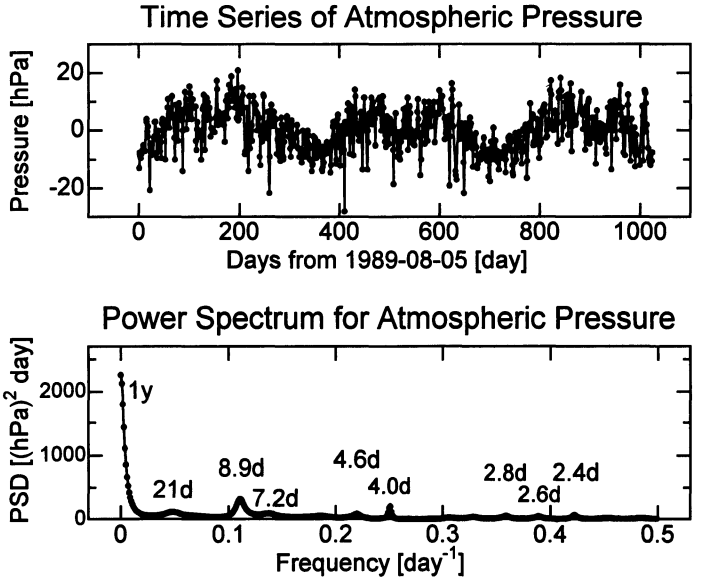

Fig. 8 Time-series analysis for atmospheric pressure.
Top : plot of deviation from average. Bottom : power spectrum deduced from autoregressive model. Strong one-year periods and weak several-day periods are seen, i.e., intermediate nature of outdoor temperature and wind speed.

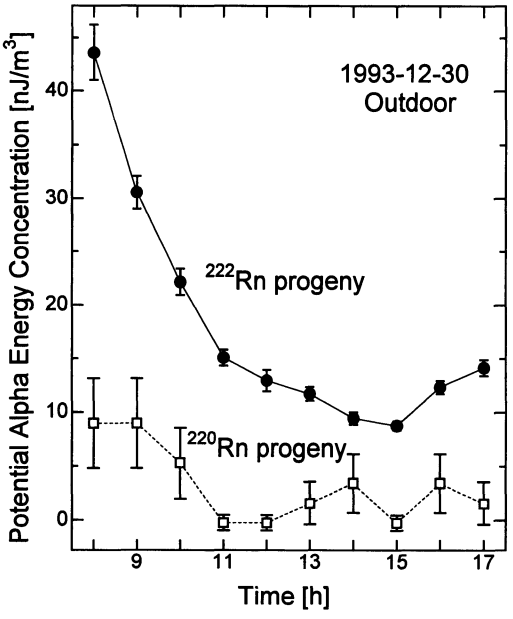

Fig. 9 Typical diurnal dependence of outdoor ^{222}Rn- and ^{220}Rn-progeny concentration.
Well-known behavior, i.e., high in the morning and low in the evening, is seen also for ^{220}Rn progeny.

$$R(\tau)=\lim_{T\to\infty}\frac{1}{T}\int_0^T x(t)x(t+\tau)\mathrm{d}t \qquad (1)$$

which represents the correlation of the two signals separated from τ. Since real data consist of a finite set of N sampled signals, $x(j)$, $j=1, 2, \cdots, N$, Eq. (1) may be rewritten in a discrete form of

$$R(i)=\frac{1}{N-i}\sum_{j=1}^{N-1}x(j)\cdot x(j+1),$$
$$i=0,1,2,\cdots,N=1. \qquad (2)$$

However, Eq. (2) is unreasonable because the reliability of $R(i)$ decreases as i increases. Therefore, taking $2N$ sampling signals, the present authors used

$$R(i)=\frac{1}{N}\sum_{j=1}^{N}x(j)\cdot x(j+1),$$
$$i=0,1,2,\cdots,N, \qquad (3)$$

where the average value was subtracted from $x(t)$, and $R(i)$ was normalized as $R(0)=1$. Although the present data have many missing values because of holidays, the reliability changes of $R(i)$ with missing values were within 30%.

Sampling a continuous signal in a finite period, τ, omits information on the time variation shorter than τ. From a view point of frequency domain, there is an upper limit in frequency component determined from the sampling period, τ. In the field of sampling theory, this frequency, f_{max}, is called Nyquist frequency, which is set equal to half the sampling frequency, τ^{-1}. In the present case $\tau=1$ d, and $f_{max}=0.5$ d^{-1}, thus the present measurement was not able to discuss about the periodicity which was shorter than 2 days.

The Fourier transform of the ACF, $R(i)$, obtained from Eq. (3), gives a power spectrum of the signal, $x(t)$. Fourier transform is defined as

$$X(\omega)=\int_{-\infty}^{\infty}x(t)\mathrm{e}^{-\mathrm{i}\omega t}\mathrm{d}t,$$
$$x(t)=\frac{1}{2\pi}\int_{-\infty}^{\infty}X(\omega)\mathrm{e}^{\mathrm{i}\omega t}\mathrm{d}\omega$$
$$(\mathrm{i}=\sqrt{-1}) \qquad (4)$$

Again, in discrete form, the input signal, $x(t)$, is sampled with a time interval of Δt. Therefore, k-th sampling value is expressed as $x_k=x(k\Delta t)$, and a discrete Fourier spectrum, $X_l(l\Delta\omega)$ is calculated as

$$X_l=\sum_{k=0}^{N-1}x_k\mathrm{e}^{-\mathrm{i}l\Delta\omega k\Delta t}\Delta t,$$
$$l=0,1,\cdots,N-1 \qquad (5)$$

where in the present case $\Delta t=1$ d and $\Delta\omega=2\pi(N\Delta t)^{-1}$[d^{-1}]. To reduce calculation time, fast Fourier transform (FFT) was used. When using FFT, N is restricted to the power of 2.

The mean square of $X(\omega)$ in Eq. (4),

$$S(\omega)=\lim_{T\to\infty}\frac{1}{T}|X(\omega)|^2 \qquad (6)$$

is the power spectrum of $x(t)$. The power spectrum, $S(\omega)$, and the ACF, $R(\tau)$, are related each other through Fourier transform:

$$S(\omega)=\int_{-\infty}^{\infty} R(\tau)\,e^{-i\omega\tau}d\tau \qquad (7)$$

which is called Wiener–Khinchin theorem.

$R(0)$, $R(1)$, $\cdots$, $R(N/2)$ were symmetrically arranged to left and right of the real part of the integrand of Eq.(7), the symmetry of the ACF being used. The real part of the result of N-point FFT was used as a power spectrum.

Besides the method which uses ACF and FFT, autoregressive model (AR) was finally used to obtain a power spectrum from a signal. AR simply assumes a model,

$$x_k=-\sum_{i=1}^{m} a_{mi}x_{k-i}+n_k \qquad (8)$$

where m is an order of AR, a_{mi} is a constant, and n_k is a stationary white noise which is independent of x_l ($l<k$). Equation (8) and, again with Wiener–Khinchin theorem, power spectrum was calculated from autocorrelation function. Spectral analysis with AR was developed by Akaike[9] in 1969, and is known to be equivalent to maximum entropy method (MEM) which Burg[10] proposed in 1967. AR (or MEM) is able to estimate power spectrum with high resolution even from a limited interval of time-series data.

References

1) Kobayashi, T. and Takaku, Y. : Estimate of effective dose equivalent from radon daughters in the natural environment of Fukushima-city, *Hoken Butsuri*, 24, 129–132 (1989) (in Japanese with English abstract)

2) Kobayashi, T. and Takaku, Y. : Measurement of atmospheric radon daughter concentrations at the campus of Fukushima Medical College, *Fukushima J. Med. Sci.*, 35, 29–43 (1989)

3) Kobayashi, T. and Takaku, Y. : Comparisons of natural radiation at new and old campus of Fukushima Medical College, *Hoken Butsuri*, 26, 117–122 (1991) (in Japanese with English abstract)

4) James, A. C., Bradford, C. F. and Howell, D. M. : Collection of unattached RaA-atoms using a wire gauge, *J. Aerosol Sci.*, 3, 243–254 (1972)

5) Marriott, F. H. C. : "A Dictionary of Statistical Terms", 5th ed. Longman (1990)

6) Minato, S. : Broad bandwidth spectral analysis of variations in the concentrations of atmospheric radon daughters. In: Environmental radon, proceedings of the '91 Radon Symposium held at Kumatori. Electron Science Institute, Japan, pp. 308–313 (1992) (in Japanese with English abstract)

7) Hino, M. : "Spectral Analysis", Asakura Shoten, Tokyo (1977) (in Japanese)

8) Minami, S. : "Wave Shape Data Processing for Scientific Measurement", CQ Shuppan (1986) (in Japanese)

9) Akaike, H. : *Annals Inst. Statist. Mathem.*, 21, 243–247 (1969)

10) Burg, J. P. : Geophys., Oklahoma City, Okla., Oct., 31 (1967)

要　旨

空気中ラドン・トロン娘核種の4年間にわたる間欠測定

小林恒夫，高久祐治

福島県立医科大学　960-12　福島市光が丘1

空気中のラドン・トロン娘核種のレベルとその動態を調べるために，福島県立医科大学において4年間，同一時刻における娘核種濃度の間欠的測定を行った。真空下でのα線スペクトロスコピィを使ったフィルタ法により，^{212}Poのピークを明瞭に分離することができた。屋内のトロン娘核種を除いて，夏低濃度で冬高濃度という明瞭な季節変動が観測された。ラドン娘核種は対数正規分布によく従ったが，トロン娘核種はポアソン分布的な分布を示した。重回帰分析と相関分析の結果，屋内のラドン娘核種は主として屋外の空気を起因とすることが判明した。時系列解析の結果，3日から9日の周期が観測されたが，これは風速の同様な周期と一致することがわかった。